



The effect of Ti and TiN barrier layers on the stress and adhesion of Cu thin films deposited on Si

D. Beegan^{1, 2}, M.T. Laugier^{1, 2} & A. Arshak^{1, 2}

¹ *Department of Physics, University of Limerick, Ireland.*

² *Materials and Surface Science Institute, University of Limerick, Ireland.*

Abstract

The effect of Ti and TiN barrier layers on the mechanical and electrical properties of RF magnetron sputtered Cu thin films is investigated. The relationship between the mechanical properties of film stress and adhesion is investigated in the two-layer film structure by indentation techniques. Changes in the length of indentation cracks are attributed to stresses in the films. Adhesion is determined from the scratch test. The resistivity of the films was measured by four-point probe and the films were characterised by AFM and XRD.

1 Introduction

Aluminium has long been the metal of choice for interconnects because of its ease of working and low resistivity. However, as devices shrink and interconnects decrease in cross-section, aluminium will soon reach the technological and physical limits for existing technology. Copper is the most suitable material to replace aluminium due to its low resistivity, high electromigration resistance, higher melting temperature and mechanical strength.

There are, however, problems with the incorporation of copper into the structure of an integrated circuit. Copper is a deep level impurity in silicon and diffuses rapidly through silicon dioxide in the presence of an electric field. This causes degradation of the transistor reliability by forming particular impurity levels in the silicon. A thin barrier layer is required to prevent the diffusion of the copper through the silicon dioxide. Titanium and titanium nitride are two materials currently being investigated for this purpose.

44 Surface Treatment

1.1 Microindentation

Indentation fracture techniques are a simple and rapid means of determining the fracture toughness of brittle materials. The model developed by Lawn and Fuller attributes changes in indentation crack lengths when a surface layer is present to stress in the surface layer [1]. This is a simple way to determine the stress in thin films on a brittle substrate. Their model predicts a change in the computed fracture toughness, K , which is independent of indenter load.

For this model to be valid the crack length must be larger than the indent impression but not too large that lateral chipping disrupts the pattern. K_c is the critical stress intensity and is written as the sum of the residual stress intensity factor K_r and the surface contribution K_s . The residual stress, K_r , is given by:

$$K_r = \frac{\chi P}{c^{3/2}}, \quad \left(\chi = 0.016 \sqrt{\frac{E}{H}} \right) \quad (1)$$

where P is the indentation load (N), c is the half-penny crack radius measured from the indentation centre, E is the Young's modulus, and H is the hardness. The empirical results for χ can be replaced with an analytical result for E/H dependency. The resulting values of K_r are however very similar [2].

K_s is the stress intensity at the crack tip, near the surface, induced by the presence of a thin stressed layer, and is given by:

$$K_s = 2\Psi \sigma_s \sqrt{d} \quad (2)$$

where Ψ is a geometry term ≈ 1 , d is the thickness of the stressed layer and σ_s is the stress. Therefore the total stress intensity factor for radial crack system is given by:

$$K = \frac{\chi P}{c^{3/2}} + 2\Psi \sigma_s d^{1/2} \quad (3)$$

For equilibrium crack conditions $K = K_c$. A more convenient form of eqn (2) may be obtained by using the reference state of zero surface stress to eliminate χ . Thus, by inserting $c = c_0$, at $\sigma_s = 0$, into eqn (2) we get:

$$\frac{2\Psi \sigma_s \sqrt{d}}{K_c} = 1 - \left(\frac{c_0}{c} \right)^{\frac{3}{2}} \quad (4)$$

where K_c is the toughness of the substrate, $c = c_0$ is the crack length in the absence of stress and c the crack length measured when a thin stressed layer is present. This equation effectively relates changes in the extent of radial cracks to the presence of a thin highly stressed layer.

1.2 Scratch testing

The scratch test is a simple and widely used method for investigating adhesion in thin films. In the scratch test a Rockwell C diamond indenter is lowered on to the sample at increasing loads as the indenter tip is moved across the surface of the sample. The critical load, L_c , needed to cause coating removal may be used directly as a measure of adhesion. There are various different modes of failure

associated with scratch testing, which have been characterised by Burnett and Rickerby [3]. Ductile coatings tend to fail by peeling, whereas brittle coatings tend to spall.

A scratch model has been formulated by Laugier [4], which relates the critical load to the work of adhesion. This approach postulates that the energy stored in the coating is responsible for generating new surfaces at the original interface. The stored energy in a length Δx of coating ahead of the indenter is expressed as:

$$\frac{[\sigma(x)]^2}{Eh\Delta x} \quad (5)$$

where h is the thickness of the coating, $\sigma(x)$ is the stress in the coating and E is the Young's modulus of the coating.

A fundamental quantity that characterises an interface is the energy required to separate a unit area of the two bonded surfaces. This maybe referred to as the thermodynamic work of adhesion, W , and is defined as $W = \gamma_1 + \gamma_2 - \gamma_{12}$, where γ_1 and γ_2 are surface energies of the coating and the substrate and γ_{12} is the interfacial energy [7]. The criterion for adhesion is obtained by equating W for debonding Δx of interface to the stored elastic energy i.e.

$$W = \frac{[\sigma(x)]^2 h}{2E} \quad (6)$$

The compressive stress ahead of the indenter is given by $\sigma = \sigma_{\text{appl}} + \sigma_{\text{int}}$, where σ_{appl} is the applied stress due to the moving indenter, and is determined by both the frictional properties of the coating/indenter interface and the mechanical properties of the substrate, and σ_{int} is the internal stress in the coating which may compressive or tensile. The applied stress resulting from the sliding indenter may be written as:

$$\sigma_{\text{applied}} = \frac{(10f-1)P^{1/3}(3E_{\text{substrate}}/4kR)^{2/3}}{4\pi} \quad (7)$$

where f is the coefficient of friction between the indenter and the coating, P is the load applied, E is the Young's modulus of the substrate, R is the radius of the indenter (200 μm) and k is a constant from Hertzian theory involving the elastic modulus of the substrate and the indenter (k for Si/Diamond = 0.52).

2 Experimental

2.1 Sample preparation

P-type silicon (100) wafers (Wacker, $\rho = 2\text{-}30\mu\Omega\text{cm}$) were used as substrates in this work. Specimen cleaning was carried out in clean room conditions. Cleaning of the wafers involved a standard 3-stage process (acetone, methanol, deionised water, hydrogen peroxide, hydrochloric acid, deionised water, hydrofluoric acid, deionised water). Finally they are dried in nitrogen. A thin layer of SiO_2 was then thermally grown on the substrates. All other films were deposited in an RF magnetron sputtering system (Leybold Lab 500, Rf 13.56MHz). The chamber base pressure was below $2.3 \times 10^{-5}\text{mbar}$ and the process pressure was 4mTorr. Barrier layers of Ti were deposited on the SiO_2 using a Ti target (99.995%) in an

46 *Surface Treatment*

Ar atmosphere using RF powers ranging from 100 to 200W. Ti films were deposited at rates of 10 to 12nm/min. TiN films were reactively sputtered using the Ti target in Ar+N₂ (20%) atmosphere. These films were deposited at RF powers of 150 and 200W, at a deposition rate of 2nm/min and deposition temperatures of ambient and 250°C. Following this thin films of Cu were sputtered with RF powers of 75, 150 and 250W using a 99.9999% pure Cu target. Cu deposition rates varied from 18 to 42nm/min. The vacuum was broken between each film deposition. An in-situ quartz crystal oscillator was used to monitor the film thickness. Tolansky's technique, a multiple-beam-interferometric method, was used to make accurate film thickness measurements.

2.2 Film Characterisation

The crystal structure of the resulting thin films was confirmed by X-ray diffraction analysis (Cu K α , 40kV, 30mA) using a Philips X-pert (Cu K α , 40kV, 30mA). The XRD measurement angle (2 θ) was in the range 20 to 140° with a 0.02° interval. Surface roughness and grain size were measured by atomic force microscopy (AFM) and film resistivity was measured using a four-point probe technique.

The indentation technique was used to investigate the residual stresses in the films. Microhardness indentations were carried out on all samples using a Leco M-400-G1 microhardness tester. Each sample was indented with loads from 10 to 500gf, with at least three indentations per load. A constant loading cycle of 15s was used for all indents.

Scratch testing was carried out to investigate the adhesion of the films. Scratch testing was carried out on all samples using the CSEMEX Revetest. The CSEMEX is a progressive loading device with a Rockwell C diamond indenter of radius 200 μ m. The load was increased from 0 to 10N in all experiments and the loading rate was set at 30N/min with a table speed of 16mm/min. The friction force is measured and a piezoelectric accelerometer detects the acoustic emissions produced as the coating is damaged. The value of the critical load is then determined using these traces in conjunction with an optical microscope. All scratches were carried out at least four times and in the same direction.

3 Results and Discussion

3.1 Film Characterisation

The thickness of the films was measured by Tolansky's technique, a multiple beam interferometry method, in which a step in the Fizeau fringes is measured. The Cu films were found to be of thickness' 125 to 540nm, with a SiO₂ layer of 100nm and the Ti and TiN interlayers range from 20 to 120nm. Fig. 1 shows the XRD spectra for Cu films on Si/SiO₂ substrates and with Ti and TiN interlayers. XRD analysis showed that the texture of the Cu films was typical for sputter-deposited copper [4], a strong (111) preferred orientation with some (200) and some smaller components i.e., (220), (311), (331) and (420). The Ti and TiN

films were only 20-40 nm thick, and consequently no Ti or TiN peaks were visible in these spectra.

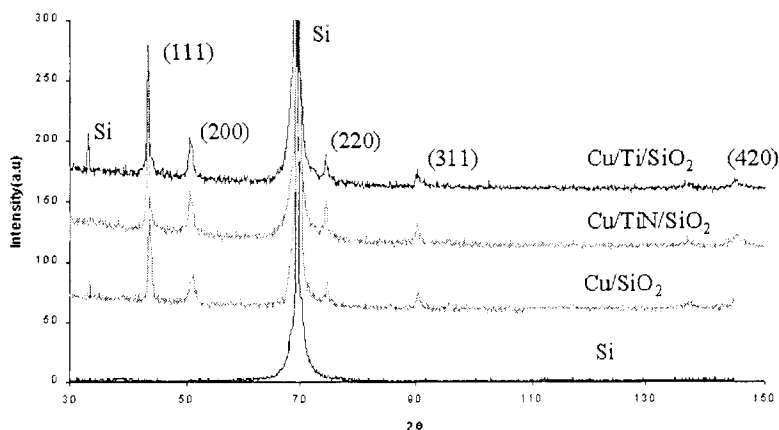


Figure 1: XRD spectra of Cu films on various substrates.

AFM was used to measure the surface roughness and grain size of the sputter deposited copper films. Samples were scanned at ranges from 80x80 to 1x1 μ m. The average surface roughness is found to vary from 2 to 8nm with the grain size varying from 40 to 100nm for these films.

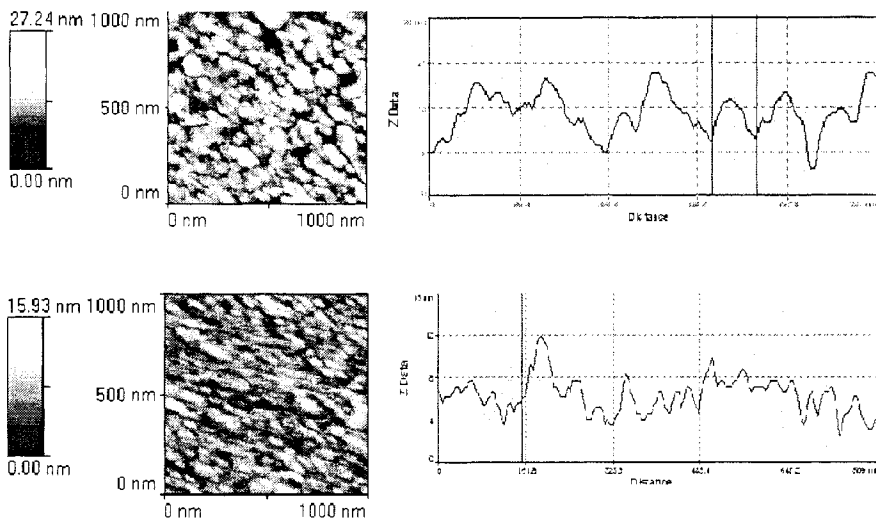


Figure 2: Copper AFM images and line scans. Scan range 1 μ m x 1 μ m.

48 Surface Treatment

Copper films deposited directly on Si were found to have a resistivity of 1.73 to 3 $\mu\Omega$ cm. These values were found to vary with thickness (see Figure 2). As the thickness of the films is increased the resistivity is found to decrease. This has also been observed previously [6]. The increase in resistivity as film thickness' decrease, is found to be more pronounced as the layer thickness approaches the mean free path of the electrons. The Mayadas-Schatzkes model concludes that thickness effects, associated with the mean free path of electrons, contribute to the variation in resistivity with metal film thickness [7]. Cu films with thickness' of 400 to 500nm deposited on SiO_2 , Ti and TiN are found to have higher resistivities of 3.5, 3.62 and 3.78 $\mu\Omega$ cm respectively.

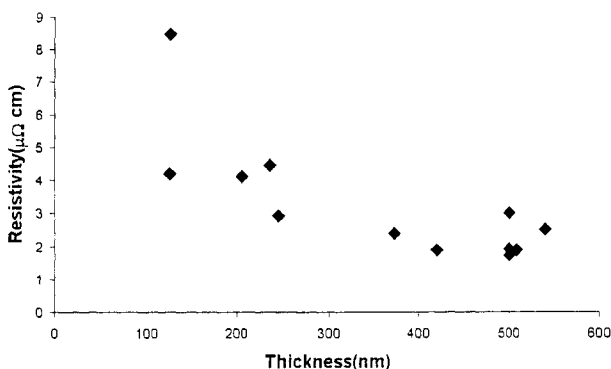


Figure 3: Variation of resistivity with thickness for Cu films on Si.

3.2 Microindentation

Si wafers were indented first to determine the hardness and toughness of the substrate and the crack length of the unstressed material. The hardness, H , was found to be 12.1GPa and the toughness, K_{IC} , was found to be 0.61MPam^{1/2}. The apparent fracture toughness values for all samples may be seen in Table. 1. From these we can see a K_{IC} for SiO_2/Si of 0.67MPam^{1/2} and values ranging from 1.1MPam^{1/2} for Cu/ SiO_2 to 1.18MPam^{1/2} for Cu/TiN.

For equation (1) to be valid the crack length must be very much larger than the indent size. Therefore the stress was calculated using the higher loads of mainly 200, 300 and 500gf, where clear crack patterns without lateral cracking were observed. The stresses calculated may be seen in Table 1. As can be seen the stress in Cu films deposited directly on a Si wafer was compressive at 495MPa. In the Cu/ SiO_2 system the compressive stress is reduced to 478MPa. The addition of Ti and TiN interlayers further decrease the stress in the multilayer system to values of 316 and 275MPa respectively. The SiO_2 films on Si substrates had compressive stress of 43MPa with the Ti/ SiO_2 and TiN/ SiO_2 systems having compressive stresses of 146 and 102MPa respectively.

In Fig. 4 we can see some of the indents on the various samples. For the Si, SiO_2 , Ti and TiN samples at the higher loads of 500gf some lateral cracking was observed. With the copper films, however, delamination of the film around the

indent may be seen. This is similar to the results of Ritter *et al* for indentation of soft polymer films on hard glass substrates [8]. They attributed the debonding to contact interfacial shear stresses at the perimeter of the contact region.

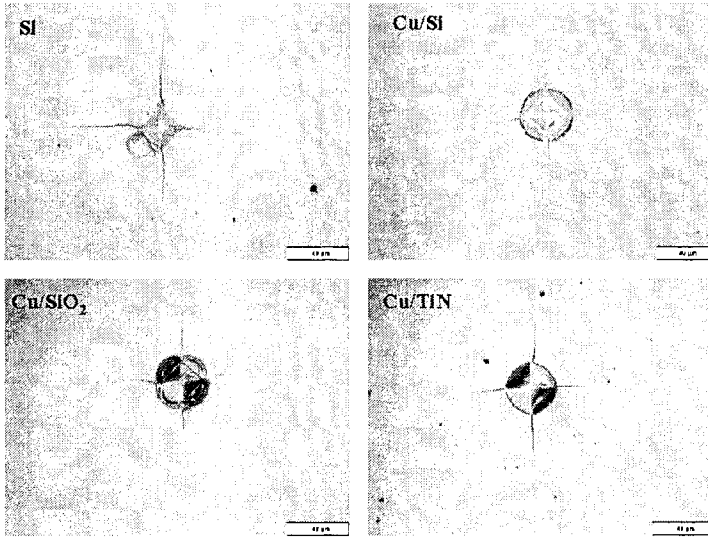


Figure 4: Microhardness indentations at 500gf

Table 1: Results

Sample	Thickness	4 point probe		Microhardness		
		$\rho(\mu\Omega \text{ cm})$	H(GPa)	$K_c(\text{MPa m}^{1/2})$	$\sigma_s(\text{Mpa})$	
Si			12.14	0.52		
SiO ₂ /Si	100		9.79	0.68	-37.73	
Cu/Si	450	2.43	10.28	1.12	-354.72	
Cu/SiO ₂	470	3.5	11.8	1.1	-300	
Cu/Ti	510	3.8	11.92	1.14	-274	
Cu/TiN	470	3.62	13.3	1.18	-238	
Ti/Si	121		13.62	0.54	34.15	
TiN/Si	20.9		12.94	0.55	-128.85	
Ti/SiO ₂	40		12.5	0.36	-126.81	
TiN/SiO ₂	40		12.22	0.55	-94.4	

3.3 Scratch testing

Scratch testing of the silicon dioxide, titanium and titanium nitride layers displayed brittle failure. Film failure occurred by spallation or chipping of the films. Cracking of the films also occurred as the indenter reached the critical loads. The copper films are ductile, however, and exhibit ductile failure modes. The films may buckle at low loads and are consequently smeared off the

50 Surface Treatment

substrate as the load is increased. The critical load for copper is taken to be the load at which the film begins to buckle or smear.

For copper films deposited directly on silicon a critical load of $7.2 \pm 0.2 \text{ N}$ is found. This load corresponds to point at which smearing of the film is first observed, as no buckling is observed on these films. The AE and frictional force trace for one such scratch is shown in Figure 5. The first peak in the AE trace corresponds to the initial scratching of the films. The second peak on the AE trace corresponds to the smearing of the film. The frictional force trace is also seen to change at these two points. The slope of this graph is seen to change as the film is first scratched. From the frictional force graph the coefficient of friction may be calculated (see Table 2).

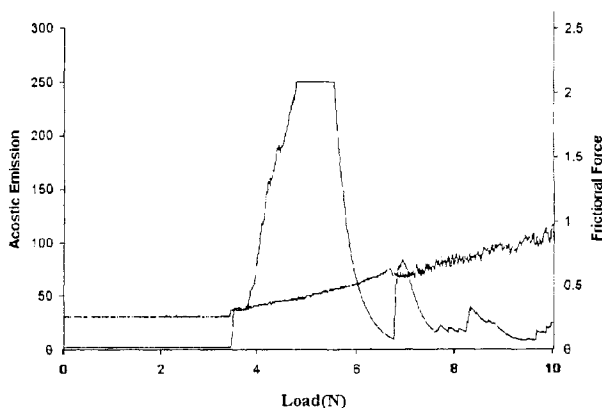


Figure 5: Acoustic Emission and Frictional Force traces

The copper films on silicon dioxide exhibit much lower adhesion. The films buckle almost immediately as the scratch is seen and at loads as low as 0.6 N the copper is smeared away to reveal the silicon dioxide layer beneath. The critical load is $1.5 \pm 0.9 \text{ N}$. The AE graph generally shows a peak almost immediately, which corresponds to the initial buckling of the film, with a second peak around 4 to 5.5 N corresponding to the smearing of the film from the substrate. As the load increases we begin to see cracking in the center of the scratch track corresponding to failure in the silicon dioxide layer.

Table 2: Scratch test results

Sample	Thickness	$L_c(\text{N})$	f	$\sigma_a(\text{GPa})$	$\sigma_s(\text{MPa})$	$\alpha_1(\text{GPa})$	$W(\text{J/m}^2)$
SiO_2/Si	100	5.10	0.24	1.61	43	1.65	1.86
Cu/Si	450	7.2	0.08		495		
Cu/SiO_2	470	1.5	0.07		478		
Cu/Ti	510	7	0.08		316		
Cu/TiN	470	9.2	0.07		275		
Ti/Si	121	8.60	0.23	1.78	-39	1.75	1.53
TiN/Si	21	8.00	0.12	0.27	148	0.42	0.07
Ti/SiO_2	40	8.9	0.22	1.66	146	1.79	1.87
TiN/SiO_2	40	8.4	0.11	0.14	102	0.24	0.05

The copper films deposited on titanium show a better adhesion than with the silicon dioxide. Although some films do buckle at low loads, overall there is little buckling or smearing of the films. Small strips of the copper appear to be removed along the edge of the scratch track corresponding to cohesive but not adhesive failure. This happens at loads greater than 6.5N. As the load increases film removal from the centre of the scratch track is observed. This point is taken to be the critical load of 7 ± 0.6 N.

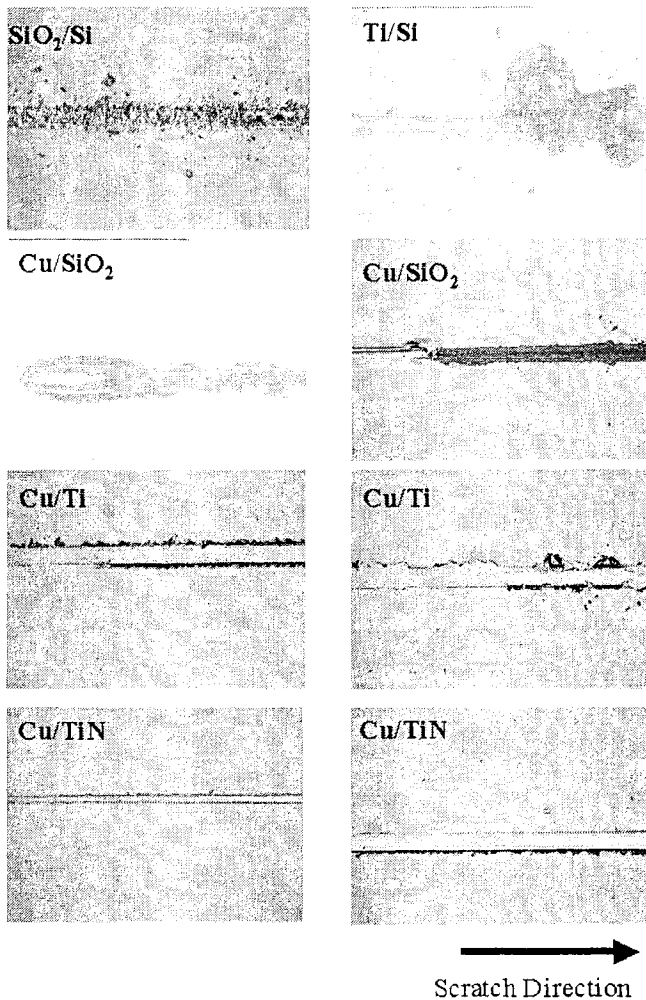


Figure 6: Scratch tracks

For Cu/TiN systems the critical load is found to be 9.2 ± 0.3 N and the films show very little evidence of failure at lower loads. The AE graphs show a small

52 Surface Treatment

peak at around 4N where the scratch is seen and at loads greater than 9N a peak is starting corresponding to the beginning of smearing of the film. For some scratches on these samples no adhesive failure is evident up to the maximum load of 10N.

The critical loads for these films may be seen in Table 2. For scratches on the SiO₂, Ti and TiN films Laugier's model may be applied to determine W_a , the work of adhesion. The values used in the calculations of W_a may be seen in Table 2. Unfortunately this model may only be used on films exhibiting brittle failure and therefore cannot be used to determine the work of adhesion for copper films. The values for the Young's modulus of Si, SiO₂, Ti and TiN are taken to be 107, 73, 120 and 250 GPa respectively [9].

4 Conclusions

The stress, resistivity and adhesion of Cu thin films RF magnetron sputtered on Si substrates with a SiO₂ dielectric layer has been investigated. The effect of Ti and TiN barrier layers on the properties of the multilayer system has also been investigated. The experiments reported here demonstrate that the adhesion of Cu films to SiO₂/Si substrates is poor, but can be enhanced by the presence of a Ti or TiN interlayer. These interlayers also reduce the compressive stresses present in the multilayer systems. Although Ti and TiN do increase the resistivity of the copper films, the values are only increased by a maximum of 2 $\mu\Omega$ cm.

Acknowledgements

The support of the Materials and Surface Science Institute (MSSI) and the Dept. of Physics at the University of Limerick was greatly appreciated during this work. Special thanks also to Syed Ansar Md. Tofail for his work on the AFM.

References

- [1] Anstis, G. R., Chantikul, P., Lawn, B. R., Marshall, D.B., *J. AM. Ceram. Soc.*, **64**, pp. 533, 1981
- [2] Laugier, M.T., A note on the elastic/plastic indentation of ceramics. *J. Mater. Sci. Letters*, **4**, pp. 1539-1541, 1985
- [3] Burnett P.J., Rickerby, D.S., The scratch adhesion test: an elastic-plastic indentation analysis. *Thin Solid Films*, **157**, pp. 233-254, 1988
- [4] Laugier, M.T., Adhesion at elevated temperatures of TiN coatings on cemented carbides, *Mat. Sci. Eng.*, **A105/106** pp. 513-516, 1988
- [5] Arnaud, L., Goneela, R., Tartavel, G., Torres, J., Gounelle, C., Gobil, Y., Morand, Y., Electromigration failure modes in damascene copper interconnects. *Micro. Rel.*, **38**, pp. 1029-1034, 1998
- [6] Mc Cusker, N.D., Gamble, H.S., Armstrong, A.M., Surface electromigration in copper interconnects. *Microelectronics Reliability*, **40** pp 69-76, 2000



- [7] Maydas, A.F., Schatzkes, M., Electrical resistivity model for polycrystalline films: the case of arbitrary reflection at external surfaces. *Phy. Rev. B.*, pp. 1382-1389, 1995
- [8] Ritter, J.E., Lardner, T.J., Rosenfeld, L., And Lin, M.R., Measurement of adhesion of thin polymer coatings by indentation, *J. Appl. Phys*, **66**(8) pp. 3626-3634, 1989
- [9] Handbook of Tables for Applied Engineering Science 2nd Edition, CRC Press